RSC Advances

ROYAL SOCIETY OF CHEMISTRY

www.rsc.org/advances

RSC advances

ARTICLE

Evaluation of polyacrylic anion exchange resins on the removal of Cr(VI) from aqueous solutions

Received 00th January 2015,
Accepted 00th January 2015

DOI: 10.1039/x0xx00000x

www.rsc.org/

Ke Xiao,[a,b] Guimei Han,[a] Jianhui Li,[a] Zhigang Dan,[a] Fuyuan Xu,[a,*] Linhua Jiang,[a,*] and Ning Duan[a]

This study evaluated the multi-cycle Cr(VI) removal performance of four polyacrylic anion exchange resins (D730, D314, 312 and 213) with different functional groups and porosities based on a fixed-bed column operation. Particular emphasis was given to the effect of oxidation fouling on the ion exchange properties and performance of polyacrylic resins. The functional groups had significant effects on the exchange capacity, adsorption rate, regeneration efficiency, and oxidative stability for Cr(VI) removal. Oxidation fouling on the polyacrylic resins had a significant influence on the removal of Cr(VI). After a 10-cycle operation, due to the oxidation of resins, the adsorption capacities of D730, 213, D314 and 312 resins decreased by 19.8, 21.7, 13.4 and 15.3%, respectively.The results of the Fourier transform infrared rays (FT-IR) analyses showed that the cleavage of C-N and C-C bonds occurred on the polyacrylic resins during the Cr(VI) removal process, indicating the degradation of resin functional group and matrix. This work provided an understanding of exchange behavior and oxidation fouling of Cr(VI) on different polyacrylic resins, and should result in more effective applications of ion exchange for Cr(VI) removal from solutions.

1. Introduction

As Cr (VI) is mobile and highly toxic in the environment, Cr(VI) removal technologies have been of great interest in recent years, including adsorption [1, 2], chemical reduction [3], biological methods [4, 5], membrane filtration [6], and ion exchange [7]. Nevertheless, many of these technologies are marginally cost-effective or difficult to implement in developing countries. The main advantages of ion-exchange are the recovery and reuse of Cr(VI), simple operation, less sludge production and the reducing Cr(VI) concentrations to near-zero levels [8].

In the past decades, various kinds of anion exchange resins were used to study the removal of Cr(VI), such as Lewatit MP 500 [9], Dowex 1×8 [10], Lewatit MP 62 [11], Lewatit MP 64 [9], Lewatit M 610 [11], Amberlite IRA 96 [10], KIP210 [8], Amberlite IRA 96 [12, 13], Amberlite IRA 400 [14], and Lewatit FO36 [15]. These studies demonstrated that better performance of the resins could be achieved in an even wide range of the initial Cr(VI) concentration from as low as 0.1 mg/L to as high as 2000 mg/L [16, 17]. However, the optimum pH for Cr (VI) adsorption was found to be in the range 1.9 – 6.0 [15], whereas at neutral to alkaline pH conditions, the Cr(VI) adsorption capacity was drastically reduced [18]. In order to obtain higher adsorption capacity of the resins, lower pH values was recommended in the literatures. It's worth noting that all the above-mentioned resins are polystyrene resins.

On the other hand, it is well known that Cr(VI) is a powerful oxidizing agent and oxidizes almost all organic materials [19], so it is often used in COD measurement [20]. Therefore, it is possible for Cr(VI) to oxidize the polymeric resins during the Cr(VI) adsorption process, which potentially alters the sorption properties of the resins. However, few studies have investigated the oxidation of polymeric resins during the removal of Cr(VI) from wastewater.

Compared with polystyrene resins, polyacrylic resins are more hydrophilic and were found to adsorb more water in dilute solutions [21], their more-open pores in the gel-phase could allow faster penetration of Cr(VI) anions. As a result, the polyacrylic resins could exhibit faster adsorption rates and higher exchange capacities than the polystyrene resins. Unfortunately, the polyacrylic resins are rarely studied in terms of the removal of Cr(VI). Moreover, different resins vary significantly in some properties, such as their functional groups and porosities, leading to distinct removal efficiencies for Cr(VI), but the effect of the resin properties on the Cr(VI) adsorption and oxidation fouling is unclear. This work elucidated the effects of the polyacrylic resin properties (functional groups and porosities) on the adsorption performance for the removal of Cr(VI), with particular emphasis on the effect of oxidation fouling during the multi-cycle operation.

[a] Technology Centre for Heavy Metal Cleaner Production Engineering, Chinese Research Academy of Environmental Sciences, Beijing 100012, China
[b] College of Water Sciences, Beijing Normal University, Beijing 100875, China
* *E-mail:* fuyuanxu@hotmail.com (F. Xu), jianglinnhuan@163.com (L. Jiang)

2. Experimental

2.1 Materials and chemicals

In this study, the polyacrylic resins in the chloride form, D730, 213, D314 and 312, were provided by Zhejiang Science and Technology Co. Ltd. The relevant physico-chemical properties and specifications of these resins supplied by the manufacturer, e.g., the functional groups, exchange capacity (q_e), etc., are summarized in Table 1. Solutions of 1 M NaOH and HCl were used for regeneration and pH adjustment. Synthetic solutions of the Cr(VI) anions (500 mg/L) were prepared by dissolving an appropriate weight of $K_2Cr_2O_7$ salt (AR grade) in distilled water.

Table 1 Characteristics properties of the anion exchange resins used in this study.

Resins	D730	213	312	D314
Matrix	Polyacrylic			
Porosity	Mac.	Gel	Gel	Mac.
Functional group	$-N^+(CH_3)_3$		$-N(CH_3)_2$	
q_e (mmol/L)	550	450	1100	1100
Granulometry (mm)	0.4-0.7	0.4-0.7	0.4-0.7	0.4-0.7
Limits of pH	1-14	1-14	1-7	1-7

2.2 Methods

The adsorption and regeneration experiments were carried out using a transparent glass column (2.8 cm i.d. × 32 cm long, with an effective column height of 30 cm, 60 g resin) at around 25 °C (Fig. 1 shows a schematic of the process). Synthetic solution (initial Cr(VI) concentration of 500 mg/L, pH of 2.0) was fed (10.4 mL/min) from the feed tank into the bottom of the glass column using a peristaltic pump then percolated upward through the resins, and was finally discharged into the corresponding effluent tanks. Samples were successively collected manually at the exit of the column at regular intervals of 1 h after the start of the experiment. When the concentration of Cr(VI) was greater than 0.5 mg/L, the regeneration of the resin was required. First, distilled water (20.0 ml/min) was fed into the column for 10 min; subsequently, 1 M NaOH solution (5.2 ml/min) was pumped until the total Cr concentration reached 0.5 mg/L; then, 1 M HCl solution (5.2 ml/min) was fed for 1 h to convert the resin to the RCl form; and finally the resin was washed with distilled water (20.0 ml/min) for 10 min. The eluate in all of the regeneration process was collected in a spent brine vessel. This test was conducted using up to 10 adsorption–regeneration cycles.

The exchange capacity (q_e) and the regeneration efficiency (R_e) of each resin were calculated by the following mass-balance equations:

$$q_e = \frac{(C_{in} - C_{e6} - C_{e3}) \times V_{eff}}{m} \quad (1)$$

$$R_e = \frac{C_{r\text{-}Cr} \times V_{eff\text{-}r}}{(C_{in} - C_{e3} - C_{e6}) \times V_{eff}} \times 100\% \quad (2)$$

where C_{in} is the initial $C_{Cr(VI)}$, mg/L; C_{e6} and C_{e3} are the Cr(VI) and Cr(III) concentrations in the effluent tanks, mg/L; V_{eff} is the volume of the produced Cr(VI) solution, L; m is the mass of resin used; $C_{r\text{-}Cr}$ is the total Cr concentration in the brine vessel, mg/L; and $V_{eff\text{-}r}$ is the solution volume of the brine vessel, L.

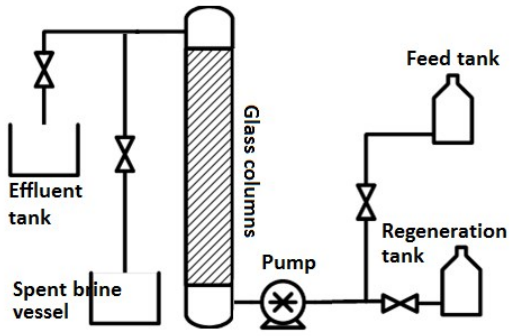

Fig. 1 Schematic process of the column system.

2.3 Chemical analyses

The colorimetric method was used to measure the concentrations of Cr(III) and Cr(VI) in the solutions [22]. The concentration of Cr(VI) was analyzed by the 1,5-diphenylcarbazide method. To estimate for total Cr, the Cr(III) was first converted to Cr(VI) by the addition of excess potassium permanganate at boiling conditions prior to the performing the 1,5-diphenylcarbazide spectrophotometric technique. The concentration of Cr(III) was calculated as the difference between the total chromium and Cr(VI) concentrations. The FT-IR spectrum of each resin was obtained using an Agilent 5500a instrument, with KBr pastilles (sample/KBr ratio of 1:100).

2.4 Quality assurance and quality control (QA/QC)

The standard curves of Cr(VI) and total Cr analyses were prepared with two series of 8-point calibrations. The linear working range of the standard curves was from 0 to 0.2 mg/L, and the concentrations of the samples under test were diluted to that of the standard curves. Excellent linear calibration was generally with a correlation coefficient of 0.9995, or better. The standard curve of total Cr was calibrated with Cr(VI) standard solution. Quality control samples were analyzed to assure that the calibrations were valid for the analysis.

3. Results and discussion

3.1 Evaluation of the breakthrough curve

The breakthrough curves, which show the exchange behaviour of the four resins in column operation, were studied. Breakthrough occurred at 0.5 mg Cr(VI)/L, approximately 148, 125, 186 and 164 bed volumes (BVs) of 500 mg Cr(VI)/L water could be treated, and the corresponding total q_e values were 103.7, 89.4, 132.3 and 116.3 mg Cr/g for the D730, 213, D314 and 312 resins, respectively (Figures not shown). To understand the breakthrough curve better for the removal of Cr(VI), the breakthrough curve model was used to describe the adsorption rate and q_e for these resins.

The development of a mathematics model that describes such breakthrough curve is difficult, since the Cr(VI) concentration in the solution, which moves across the column, continuously changes. The fundamental models for a fixed-bed column depend on the mechanism responsible for the mass transfer from the solution to the resin surface, the diffusion on the surface of the resin, and rates of these processes, etc. Recently, various breakthrough curve models such as bed-depth/service time analysis (BDST), Adams–Bohart, Thomas, Yoon and Nelson and Mass transfer models have been developed to predict the dynamic behaviour of the column and allow some kinetic coefficients to be estimated [23]. The Yoon-Nelson model is relatively simple and requires little detailed data concerning the characteristics of the adsorbate, the type of adsorbent, and the physical properties of the adsorption bed, but it can predict the breakthrough curve in the column-adsorption process [23, 24]. The Yoon-Nelson model for a single-component system is expressed as:

$$\frac{C_{e6}}{C_{in}} = \frac{1}{1+e^{K_{YN}(\tau - t)}} \quad (3)$$

where K_{YN} is the rate constant (min^{-1}), τ is the time required for 50% adsorbate breakthrough (min) and t is the breakthrough time (min). The linearized form of the Yoon-Nelson model is as follows:

$$\ln \frac{C_{in} - C_{e6}}{C_{e6}} = \frac{1}{K_{YN}t - K_{YN}\tau} \quad (4)$$

Based on Eq. (4), the parameters K_{YN} and τ for the resins were investigated, and these parameters have been discussed in some studies of the adsorption of metal ions using varied adsorbents by the linear graph of adsorption time (t) versus $\ln[C_{e6}/(C_{in}-C_{e6})]$ [23, 25]. τ was defined as 50% breakthrough of the sorption process, so the resins should be completely saturated at 2τ. Due to the symmetrical nature of the breakthrough curve, the amount of Cr(VI) adsorbed by the resins is one half of the total Cr(VI) entering the adsorption column within the 2τ period [24]. Hence, the following equation can be written:

$$q_0 = \frac{\frac{1}{2}C_{in}v(2\tau)}{m} = \frac{C_{in}v\tau}{m} \quad (5)$$

where q_0 is the predicted exchange capacity (mg/g), v is the liquid flow rate (ml/min), and m is the amount of the resin in the column (g).

The Yoon-Nelson model describes the sorption rate constant (K_{YN}) and q_0 well, according to the correlation coefficient (R^2), which is shown in Table 2. The q_0 predicted by the Yoon-Nelson model was close to the experimental data for these resins. The D314 resin has the highest value for q_0 at equilibrium. The relative q_0 values of the other resins are q_0 (D314) = 1.11q_0 (312) = 1.27q_0 (D730) = 1.45q_0 (213). The Yoon-Nelson constant, K_{YN}, which can be related to the adsorption rate for these resins, was in the order of K_{YN} (D730) > K_{YN} (213) > K_{YN} (312) > K_{YN} (D314).

Table 2 Kinetic parameters of Yoon-Nelson model for Cr(VI) sorption on the four resins.

Resins	Yoon-Nelson model parameter		
	$K_{YN}(min^{-1})$	q_0(mg/g)	R^2
D730	0.017	108.63	0.951
213	0.015	94.25	0.948
D314	0.010	137.81	0.937
312	0.012	124.37	0.917

From Table 2, both of the q_e and adsorption rate of the anion exchange resins were influenced by the functional groups. For example, the total q_e of the D730 and 213 resins were 108.6 and 94.3 mgCr/g, which were much higher than their ion-exchange capacities given by the manufacturer as 550 and 450 mmol/L resin (equal to 96.3 and 79.3 mgCr/g resin) (Table 1), respectively. This difference in the q_e might be due to the functional groups of the resins and the forms of the Cr(VI) anions. As the functional groups of the D730 and 213 resins have charges, multilayer adsorption of Cr(VI) can occur, and $Cr_3O_{10}^{2-}$ or $Cr_4O_{13}^{2-}$, which are formed on the anion exchange sites due to the high concentration of Cr(VI) [21], can be adsorbed. Meantime, the adsorption rates of the D730 and 213 resins were faster than those of the D314 and 312 resins. Previous studies have shown that the adsorption rate strongly depends on the ion mobility, charge, weight of the ion, and the pH value of the solution [26, 27]. The D730, 213， D314 and 312 resins were studied under the same conditions. However, their functional groups were different, so the charges on the functional groups enhanced the interaction of Cr(VI) with the binding sites of D730 and 213 resins by greater attractive forces than with D314 and 312, resulting in much faster diffusion of Cr(VI) ions into the anion-exchange sites.

It is well known that the macroporous resins are quite different in physical morphology from gel resins. A single macroporous ion exchange particle may be viewed as an ensemble of tiny microgels with an interconnected network of pores (10-100 nm), while gel resins can be viewed as homogeneous solid phases without any significant pores in between, and only micropores (less than 2 nm) form after the resin is saturated [28, 29]. Therefore, it was anticipated that the sorption of Cr(VI) onto the macroporous resin would be faster than onto the gel resin due to the larger pores of the macroporous resin, but our results showed that the sorption rate had little relationship with the resin porosity. For the weak-base resins, the gel resin 312 had a faster sorption rate for Cr(VI) than the macroporous resin D314, which were contrary to those for the strong-base resins (Table 2). This can result from the higher concentration of Cr(VI) which improves the solid-liquid mass transfer efficiency in this study.

3.2 Cr(III) in the effluent

Cr(VI) is a powerful oxidizer, which makes it easily reduced to Cr(III) [30], as shown in the following equation [31]:

$$Cr_2O_7^{2-} + 14H^+ + 6e^- \Leftrightarrow 2Cr^{3+} + 7H_2O \quad (6)$$

In the oxidation process, the electrons are consumed, which are possibly supplied from the resins, resulting in the oxidation of the organic compounds of the resins. As shown in Eq. (6), the quantity of Cr(III) generated is in proportion to the depletion of electrons, which can reflect the quantity of the oxidized organic compounds on the resins to some extent.

To evaluate the effect of Cr(VI) oxidation on the four resins, Cr(III) was also measured in the adsorption process at regular intervals of 1 h for the first cycle, as shown in Fig. 2. The Cr(III), which was not initially present, appeared in the effluent and increased in the Cr(VI) adsorption process. From Fig. 2, it can be seen that the Cr(VI) was reduced to Cr(III) when started the sorption process. And then the concentration of Cr(III) increased sharply until about 30 BVs for the D730 and 213 resins, while that of the D314 and 312 resins increased steady. The discharge of total Cr, including Cr(III) and Cr(VI), to surface water is regulated to below 2 mg/L by the U.S. EPA [19]. When the total Cr concentration in the effluent reached 2 mg/L, approximately 23, 31, 70 and 52 BVs of 500 mgCr(VI)/L water could be treated, which were 84, 75, 62 and 68% less than that of the breakthrough point of 0.5 mgCr(VI)/L for the D730, 213, D314 and 312 resins, respectively. Therefore, the reduction of Cr(VI) by the resins is imperative to be slowed down to meet the discharge levels.

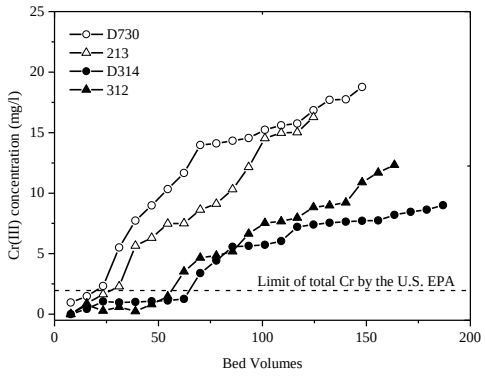

Fig. 2 Breakthrough curves of Cr(III) via the polyacrylic resins in column run at room temperature, initial Cr(VI) concentration 500 mg/L, pH 2.0 and flow rate of 10.4 ml/min.

The $C_{Cr(III)}$ in effluent tanks was also measured when the adsorption ended for every cycle, as shown in Fig. 3. The $C_{Cr(III)}$ of each resin increased with the increasing cycles, but the increase amplitude was not great. The average $C_{Cr(III)}$ of the D730, 213, D314 and 312 resins were found at 19.7, 17.2, 9.2, and 11.4 mg/L for 10 consecutive cycles operation, respectively. It can be seen that the $C_{Cr(III)}$ of the strong-base resins (D730 and 213) were higher than that of the weak-base resins (D314 and 312) in all of the cycles. It can be deduced that the functional groups greatly influenced the chemical stability of the resins.

The results presented in Fig. 2 and 3 showed the faster Cr(VI) reduction on the strong-base resins (D730 and 213) compared to that on the weak-base resins (D314 and 312), regardless of the resin porosity. For the strong-base resins, the presence of the quaternary nitrogen atoms greatly influenced the chemical stability [32]. For the gel weak-base resin (312), the $C_{Cr(III)}$ in effluent tank was higher than for the macroporous weak-base resin (D314) (Fig. 3). Rather, the $C_{Cr(III)}$ in the effluent from the gel strong-base resin (213) was lower than for the macroporous strong-base resin (D730). It can be deduced that the strong-base functional groups were more easily to be oxidized, and the porosity had little influence on the oxidative stability of the polyacrylic resins in this study.

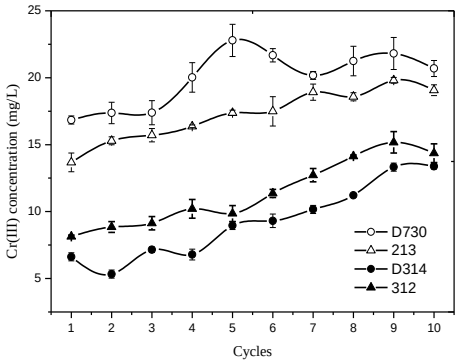

Fig. 3 Effects of cycles on Cr(III) concentration of all the resins. Column run at room temperature, initial Cr(VI) concentration 500 mg/L, pH 2.0, and flow rate of 10.4 ml/min. Symbols are average of triplicates and error bars are one standard deviation.

3.3 Regeneration efficiency

To implement a cost-effective resin for removing Cr(VI) from wastewater, it is important to assess the changes of the regeneration efficiency after an extended column operation for further use. The values of regeneration efficiency, which were evaluated by performing adsorption–regeneration experiments for 10 consecutive cycles for each resin, are shown in Fig. 4. The regeneration efficiency fluctuated in a narrow range for each resin, and the regeneration efficiencies of the weak-base resins (D314 and 312) were higher than those of the strong-base resins (D730 and 213). For the weak-base resins, according to a chromium mass balance, more than 93% of the total chromate was recovered with less than 24 BVs of eluate. However, more than 35 BVs of eluate were produced to recover less than 93% of the total chromate in the regeneration process for the strong-base resins. The average total eluate volume was 35.3 and 36.7 BVs for the D730 and 213 resins and 21.6 and 22.8 BVs for the D314 and 312 resins. These results indicated that the weak-base resins were regenerated more effectively than the strong-base resins in these experiments. Since the functional groups of the D730 and 213 resins have charges, the greater attractive forces between Cr(VI) and binding sites with charges makes it difficult to desorb Cr(VI) ions from the spent resins via ion exchange. This phenomenon explains the lower regeneration efficiencies observed for the strong-base resins than those of the weak-base resins, as shown in Fig. 4.

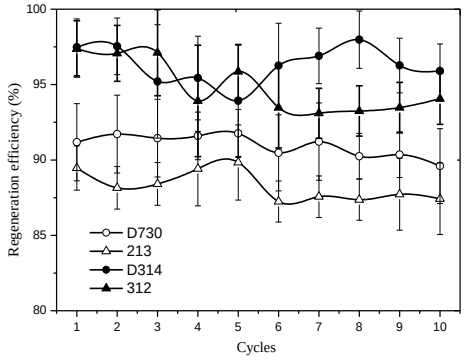

Fig. 4 The regeneration efficiency of each resin over 10 cycles. Column run at room temperature, pH of 2.0, initial Cr(VI) concentration 500 mg/L and flow rate of 10.4 ml/min. Symbols are average of triplicates and error bars are one standard deviation.

3.4 Exchange capacity

The values of q_e of the four resins for 10 cycles are shown in Fig. 5. Throughout the initial cycles, the q_e values of the D730 and 213 resins for Cr(VI) removal decreased sharply with increased cycle time and then continuously decreased slightly. For the weak-base resins (D314 and 312), the q_e decreased slightly for all of the cycles. After operating for 10 cycles, the q_e values remained at 83.2, 70.0, 114.6 and 98.9 mg Cr/g, 19.8, 21.7, 13.4 and 15.3% less than that of the first cycle for the D730, 213, D314 and 312 resins, respectively. The decrease in q_e for the strong-base resins was higher than for the weak-base resins. Generally, a decrease in q_e indicates the loss of effective functional groups, which may be mainly caused by the lower regeneration efficiency and the oxidation of resins in this experiment. The decrease in q_e for the weak-base resins that were regenerated effectively was mainly due to the oxidation of functional groups, while the decrease for strong-base resins was due to both the lower regeneration efficiency and the oxidation of functional groups.

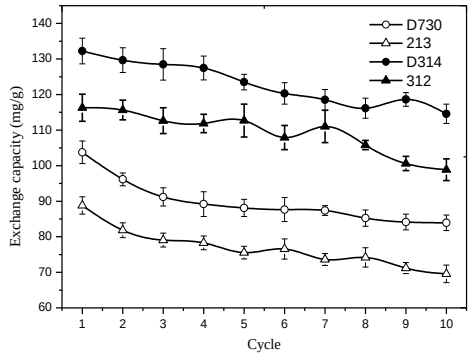

Fig. 5 Effect of the cycles on the adsorption capacity for the polystyrene resins. Column run at room temperature, initial Cr(VI) concentration 500 mg/L, pH 2.0 and flow rate of 10.4 ml/min. Symbols are average of triplicates and error bars are one standard deviation.

3.5 Changes of the effective size

To verify the changes to the polymer matrix, the volume of the resin in the effective size range (0.4-0.7 mm) was measured by wet sieve analysis before (original) and after (used) 10 cycles running (Fig. 6). The polymer matrix decomposed, as shown by the decreases in the amount of resin in the effective size range, 11.8, 12.4, 13.1 and 14.9% after 10 cycles for the D730, 213, D314 and 312 resins, respectively. Therefore, it can be concluded that some of the carbon chains of polyacrylic resin were cleaved under the oxidation of Cr(VI), resulting that the polyacrylic matrix was degraded into smaller units and discharged into the solutions, further resulting the decomposition of the resin polymer matrix.

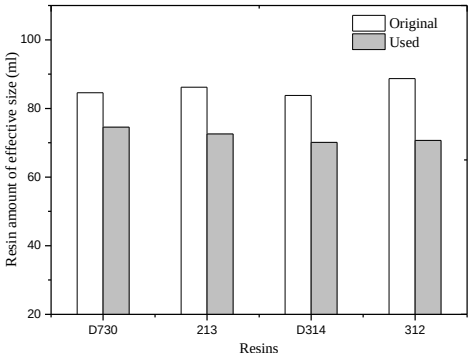

Fig. 6 Change of resin amount in the effective size range after 10 cycles.

After running for 10 cycles, the amount of the gel weak-base resin (312) in the effective size range decreased by 14.9%, which was also greater than that of the macroporous weak-base resin (D314) (Fig. 6). The same results applied to the strong-base resins (D730 and 213). That is, the oxidative stability of the macroporous matrix is better than that of the gel matrix under the same conditions.

3.6 FT-IR Analyses

In consideration of the high concentration of Cr(III) in the effluent (Fig.2 and 3), only the D730 resin was used to further clarify the changes of the groups on the polyacrylic resins. FT-IR spectra of the D730 resin were obtained at the start and end of the 10-cycle operation (Fig. 7). The main characteristic bands in the spectrum for the resin were observed at 1651-1593 cm^{-1}, 1255cm^{-1}, 1700-1800 cm^{-1} and 1460-1326 cm^{-1}, which were attributed to the stretching of C-C, stretching of C-N, C=O and the deformation of the C-H bonds respectively[33-35]. The intensity of the band at 1255 cm^{-1} (C-N) and 1617cm^{-1} (C-C) decreased after the 10-cycle operation. And the intensity of the band at 1483 cm^{-1} (-$N^{+}(CH_3)_3$) for the functional groups of the D730 resin decreased after the 10-cycle operation (Fig. 7) [7, 32].These changes in the bands for the D730 resin indicated that some of the C–C and C–N bonds were cleaved, resulting that the polyacrylic matrix was degraded and the functional groups were oxidized off the resins. On the basis of the FT-IR analyses, the oxidation mechanism of the D730 resin is proposed as shown in Fig.8.

As the C-N bonds connected with resin matrix and the functional groups are the polar covalent bonds, the positively charged nitrogen atom in the C-N bond of the strong-base resins can be the destination for electron movement, resulting that the C-N bonds which have charges on the N-containing groups are broken easily than those of the weak-base resins without charges [36, 37]. This explains the higher $C_{Cr(III)}$ of the strong-base resins than those of the weak-base resins, as shown in Fig. 2 and 3. In this study, some of the strong-base groups may be degraded off the resin matrix resulting in a sharp decrease of the exchange capacity of the strong-base resin (Fig. 5).

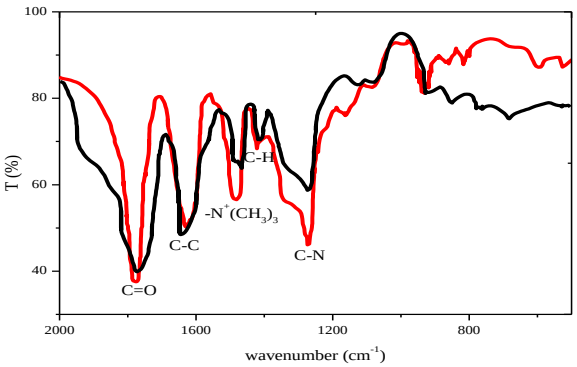

Fig. 7 FT-IR spectra of the D730 resin before (red line) and after a 10-cycle operation (black line).

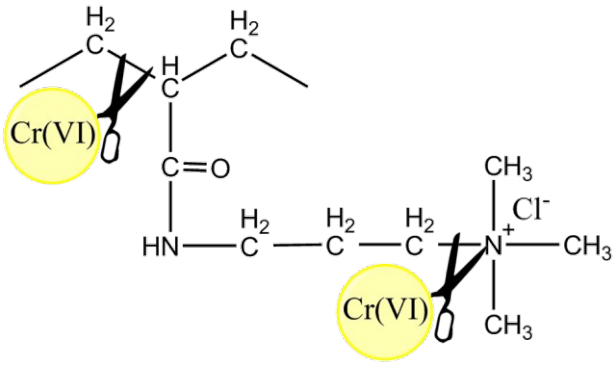

Fig. 8 The proposed oxidation mechanisms for the polyacrylic resins.

3.7 Comparison of polyacrylic resins with polystyrene resins

Table 3 summaries the comparison of the maximum exchange capacities of various polystyrene resins. These comparisons show that polyacrylic resins have higher exchange capacities than Amberlite IRA96 [10], Dowex 1×8 [10], Lewatit MP64 [9], Lewatit MP500 [9], Lewatit MP62 [11], Lewatit M610 [11], Amberlite IRA400 [14], Ceralite IRA400 [38] and Lewatit FO36 [15]. The polystyrene resin D301 [39] had higher adsorption capacity than polyacrylic resins used in this study. The easy availability and cost effectiveness of polyacrylic resins are additional advantages, which make them better sorbents for treatment of Cr(VI)-containing wastewater.

Table 3 Comparison of maximum exchange capacities of polyacrylic resins with polystyrene resins.

Polystyrene resins	q_{max} (mg/g)	pH	Reference
Amberlite IRA96	23.9	3	10
Dowex 1×8	28.0	3	10
Lewatit MP64	67.6	5	9
Lewatit MP500	57.2	6	9
Lewatit MP62	20.8	4-5.5	11
Lewatit M610	21.3	4-5.5	11
Amberlite IRA96	15.9	1.96	12
Amberlite IRA400	16.6	3-3.5	14
Lewatit FO36	15.1	6	15
Ceralite IRA400	46	2	38
D301	152.5	3	39

4. Conclusions

This is the first study to evaluate the effect of multi-cycle Cr(VI) removal on polyacrylic anion exchange resin properties and performance based on a fixed-bed column. Polyacrylic anion exchange resins were found to be effective for removing Cr(VI) from synthetic wastewater, and their adsorption performances for and oxidative stabilities against Cr(VI) mainly depended on the resin properties. The functional groups are the most critical factors that affect the adsorption rate, adsorption capacity, regeneration efficiency and oxidative stability. The obvious oxidation fouling of Cr(VI) on the polyacrylic resins had a significant influence on the Cr(VI) removal and resin properties during the multi-cycle operation. As high Cr(VI) removal and regeneration efficiencies and low concentration of Cr(III) in the effluent achieved, the macroporous weak-base resin (D314) was found to be the best one among the four polyacrylic anion exchange resins examined. In future, it is necessary to study the oxidation mechanism of the polyacrylic resins to suppress or slow down the loss of adsorption capacities and increase durability of the resins used on the treatment of Cr(VI)-containing wastewater.

Acknowledgements

This work was supported by National Natural Science Foundation of China (51304178), Major Science and Technology Program for Water Pollution Control and Treatment (2010ZX07212-006), National "Twelfth Five-Year" Plan for Science and Technology Support (2012BAF03B03), and the Funds of State Key Laboratory of Environmental Criteria and Risk Assessment (SKLECRA201555 and SKLECRA201514).

Notes and references

1. F.-y. Guo, Y.-g. Liu, H. Wang, G.-m. Zeng, X.-j. Hu, B.-h. Zheng, T.-t. Li, X.-f. Tan, S.-f. Wang and M.-m. Zhang, *RSC Advances*, 2015, **5**, 45384-45392.
2. Z. Lei, S. Zhai, J. Lv, Y. Fan, Q. An and Z. Xiao, *RSC Advances*, 2015, **5**, 77932-77941.

3. H. Wang, X. Yuan, Y. Wu, X. Chen, L. Leng and G. Zeng, *RSC Advances*, 2015, **5**, 32531-32535.
4. M. Tandukar, S. J. Huber, T. Onodera and S. G. Pavlostathis, *Environ. Sci. Technol.*, 2009, **43**, 8159-8165.
5. J. Augustynowicz, M. Grosicki, E. Hanus-Fajerska, M. Lekka, A. Waloszek and H. Koloczek, *Chemosphere*, 2010, **79**, 1077-1083.
6. B. Barikbin, S. B. Mortazavi and G. Moussavi, *Desalination and Water Treatment*, 2015, **53**, 1895-1901.
7. O. Kusku, B. L. Rivas, B. F. Urbano, M. Arda, N. Kabay and M. Bryjak, *J. Chem. Technol. Biotechnol.*, 2014, **89**, 851-857.
8. J. Yang, M. Yu and T. Qiu, *J. Ind. Eng. Chem.*, 2014, **20**, 480-486.
9. E. Pehlivan and S. Cetin, *J. Hazard. Mater.*, 2009, **163**, 448-453.
10. S. Edebali and E. Pehlivan, *Chem. Eng. J.*, 2010, **161**, 161-166.
11. F. Gode and E. Pehlivan, *J. Hazard. Mater.*, 2005, **119**, 175-182.
12. S. Bajpai, A. Dey, M. K. Jha, S. K. Gupta and A. Gupta, *Int. J. Environ. Sci. Technol.*, 2012, **9**, 683-690.
13. S. Bajpai, S. K. Gupta, A. Dey, M. K. Jha, V. Bajpai, S. Joshi and A. Gupta, *J. Hazard. Mater.*, 2012, **227**, 436-444.
14. S. Mustafa, T. Ahmad, A. Naeem, K. H. Shah and M. Waseem, *Water Air and Soil Pollution*, 2010, **210**, 43-50.
15. L. Rafati, A. H. Mahvi, A. R. Asgari and S. S. Hosseini, *Int. J. Environ. Sci. Technol.*, 2010, **7**, 147-156.
16. B. Galan, D. Castaneda and I. Ortiz, *Water Res.*, 2005, **39**, 4317-4324.
17. G. Wojcik, V. Neagu and I. Bunia, *J. Hazard. Mater.*, 2011, **190**, 544-552.
18. A. N. Siyal and S. Q. Memon, *Polish Journal of Chemical Technology*, 2012, **14**, 21-28.
19. D. Park, Y.-S. Yun, C. K. Ahn and J. M. Park, *Chemosphere*, 2007, **66**, 939-946.
20. C. E. Domini, M. Hidalgo, F. Marken and A. Canals, *Anal. Chim. Acta*, 2006, **569**, 275-276.
21. S. Deng, Q. Yu, J. Huang and G. Yu, *Water Res.*, 2010, **44**, 5188-5195.
22. F. W. Gilcreas, *American Journal of Public Health & the Nations Health*, 2012, **56**, 113-X.
23. S. H. Hasan, D. Ranjan and M. Talat, *J. Hazard. Mater.*, 2010, **181**, 1134-1142.
24. N. Ozturk and D. Kavak, *J. Hazard. Mater.*, 2005, **127**, 81-88.
25. M. Calero, F. Hernainz, G. Blazquez, G. Tenorio and M. A. Martin-Lara, *J. Hazard. Mater.*, 2009, **171**, 886-893.
26. I. Untea, E. Tudorache and V. Neagu, *J. Appl. Polym. Sci.*, 2002, **86**, 2093-2098.
27. V. Neagu, I. Untea, E. Tudorache and C. Orbeci, *J. Appl. Polym. Sci.*, 2004, **93**, 1957-1963.
28. P. Li and A. K. SenGupta, *React. Funct. Polym.*, 2000, **44**, 273-287.
29. P. Li and A. K. Sengupta, *Environ. Sci. Technol.*, 2000, **34**, 5193-5200.
30. D. Chen, K. Yang, H. Wang, J. Zhou and H. Zhang, *RSC Advances*, 2015, **5**, 65068-65073.
31. I. M. Dittert, H. d. L. Brandao, F. Pina, E. A. B. da Silva, S. M. A. G. U. de Souza, A. A. U. de Souza, C. M. S. Botelho, R. A. R. Boaventura and V. J. P. Vilar, *Chem. Eng. J.*, 2014, **237**, 443-454.
32. V. Neagu, I. Bunia and I. Plesca, *Polym. Degrad. Stab.*, 2000, **70**, 463-468.
33. S. Kalidhasan, A. S. K. Kumar, V. Rajesh and N. Rajesh, *J. Hazard. Mater.*, 2012, **213**, 249-257.
34. W. Yu, L. Zhang, H. Wang and L. Chai, *J. Hazard. Mater.*, 2013, **260**, 789-795.
35. B. R. Araujo, J. O. M. Reis, E. I. P. Rezende, A. S. Mangrich, A. Wisniewski, Jr., D. P. Dick and L. P. C. Romao, *Journal of Environmental Management*, 2013, **129**, 216-223.
36. P. Vollhardt and N. Schore, 2011, 2-6.
37. A. A. Zagorodni, D. L. Kotova and V. F. Selemenev, *React. Funct. Polym.*, 2002, **53**, 157-171.
38. P. S. Kumar, K. Kirthika and K. S. Kumar, *Adsorpt. Sci. Technol.*, 2008, **26**, 693-703.
39. T. Shi, Z. Wang, Y. Liu, S. Jia and D. Changming, *J. Hazard. Mater.*, 2009, **161**, 900-906.

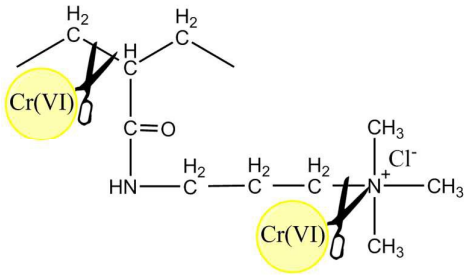

The polyacrylic resin is oxidized by Cr(VI) anions, resulting in the decrease of exchange capacity and degradation of resin matrix.